



OPEN

Allosteric coupling activation mechanism in histidine kinases

Juan Cruz Almada^{1,4}, Ana Bortolotti^{1,4}, Lucía Porrini¹, Daniela Albanesi^{1,2}, Virginia Miguel³ & Larisa Cybulski¹✉

Histidine kinases (HKs) are crucial regulators of cellular functions, mediating the phosphorylation of specific proteins to modulate their activity and localization. Upon signal detection, HKs transfer a phosphate group from ATP to a conserved histidine residue within their Dimerization and Histidine phosphotransfer domain, subsequently passing the phosphate to a response regulator (RR) that typically interacts with DNA promoters to regulate gene expression. This study investigates the signal transduction mechanism of *Bacillus subtilis* HK DesK. We generated substitutions on the conserved phospho-acceptor histidine and evaluated their effects on DesK's activity in both *in vivo* and *in vitro* contexts. Notably, we found that a variant of DesK lacking the conserved histidine could still activate gene expression. Furthermore, computational simulations of DesK variants complexed with DesR revealed interactions that could be required to maintain DesR's active conformation. Our findings elucidate an alternative pathway for RR activation via an allosteric mechanism that operates independently of histidine phosphorylation. We also demonstrated that *Escherichia coli* HK EnvZ, when lacking the conserved histidine, can activate gene expression. This HK-Allosteric Coupling Activation Mechanism functions without reliance on phosphorylation or ATP consumption, potentially serving as a fail-safe mechanism under nutrient-limited conditions.

Keywords Histidine kinase, Bacterial signal transduction, Allosteric regulation, Protein phosphorylation, Protein–protein interaction, Two-component system, Allosteric coupling activation

Protein phosphorylation stands out as a key modification enabling cells to regulate different processes, such as metabolism, development, cell division and communication, across both prokaryotic and eukaryotic organisms. This vital energy-requiring reaction is mainly catalyzed by kinases, enzymes that transfer a phosphoryl group from an ATP molecule to a protein, thereby triggering modifications in their folding, interactions, activity or localization. Histidine kinases (HKs) are the main kinases found in bacteria, but are also present in fungi and plants. Most HKs are transmembrane proteins which serve as antennas that collect relevant environmental information to elaborate an adaptive response. The ability to combine sensing and catalysis within the same protein is where the essence of HKs lies. Sensing is usually carried out by an extracellular or transmembrane domain, while catalysis takes place in the intracellular soluble domain. When an external stimulus triggers activation, a cognate biological response is mounted, most commonly involving the expression of specific genes whose products adapt the organism to the new environmental condition^{1,2}.

Widely acknowledged studies both *in vivo* and *in vitro* have demonstrated that upon activation HKs undergo autophosphorylation, thereby acquiring the phosphotransfer state^{3,4}. This state enables transferring the phosphoryl group to a partner protein known as the Response Regulator (RR). In most instances, the phosphorylation of the conserved aspartate within the receiver (REC) domain of the RR serves to promote or stabilize its active conformation. Once in this conformation, the DNA-binding domain of the RR becomes exposed, facilitating its binding to specific DNA promoters and subsequently modulating gene expression^{5,6}. Interestingly, DesR and OmpR, the RRs of the two component systems DesK/DesR and EnvZ/OmpR, respectively, have been observed to become active through a non-canonical mechanism that requires the HK but not the phosphoryl transfer from the HK to the RR^{7–9}. However, the allosteric mechanism underlying activation without phosphorylation in their corresponding kinase counterparts is still a matter that needs investigation.

¹Departamento de Microbiología, Facultad de Ciencias Bioquímicas y Farmacéuticas, Universidad Nacional de Rosario, CONICET, Rosario, Argentina. ²Laboratorio de Microbiología Molecular, Instituto de Biología Molecular y Celular de Rosario (IBR), CONICET, Universidad Nacional de Rosario, Rosario, Argentina. ³Instituto de Investigaciones Biológicas y Tecnológica (IIBYT), CONICET, Cátedra de Química Biológica, Departamento de Química, Facultad de Ciencias Exactas, Físicas y Naturales, Universidad Nacional de Córdoba, Córdoba, Argentina. ⁴Juan Cruz Almada and Ana Bortolotti have contributed equally to this work. ✉email: cybulski@rosario-conicet.gov.ar

The initial investigations recognizing histidine as the phosphorylated residue in bacterial kinases involved incubating the purified catalytic domain of *Escherichia coli* EnvZ with $\gamma^{32}\text{P}$ -ATP, followed by proteolysis¹⁰. Subsequent identification of resulting peptides through reverse-phase chromatography revealed the presence of a phosphorylated histidine (His 243) within the peptide MAGVSHDLRTP, situated within the Dimerization Histidine phosphotransfer (DHp) domain. However, the presence of other unstable or short-lived phosphorylated residues cannot be ruled out, as they may have been dephosphorylated during the pre-chromatography treatment. Furthermore, comprehensive bioinformatic analysis illustrated the high conservation of this residue among bacterial kinases.

In vivo assays provided empirical evidence corroborating the role of phosphorylation at His 243 in signal transduction, as its substitution with valine (H243V) resulted in the deactivation of EnvZ kinase activity. Consequently, subsequent investigations on other bacterial HKs were significantly influenced by these pivotal findings. Approaches aimed at identifying the catalytic residue in other kinases were consequently directed towards mutating the conserved histidine residue within the DHp domain. These investigations demonstrated that substitution of the conserved histidine with valine or alanine, which are hydrophobic and non-phosphorylatable residues, led to the loss of kinase activity in several HKs^{11–14}.

The thermosensor DesK is an illustration of a HK that belongs to the Two Component System (TCS) DesK-DesR in the Gram-Positive bacterium *Bacillus subtilis*, and whose sensing mechanism has been widely studied (described in Fig. 1A). DesK His 188 has been identified as the phosphorylatable residue by sequence homology with His 243 of EnvZ (Fig. 1B, 12,15). It was reported that phosphorylation of the conserved His was key to turn

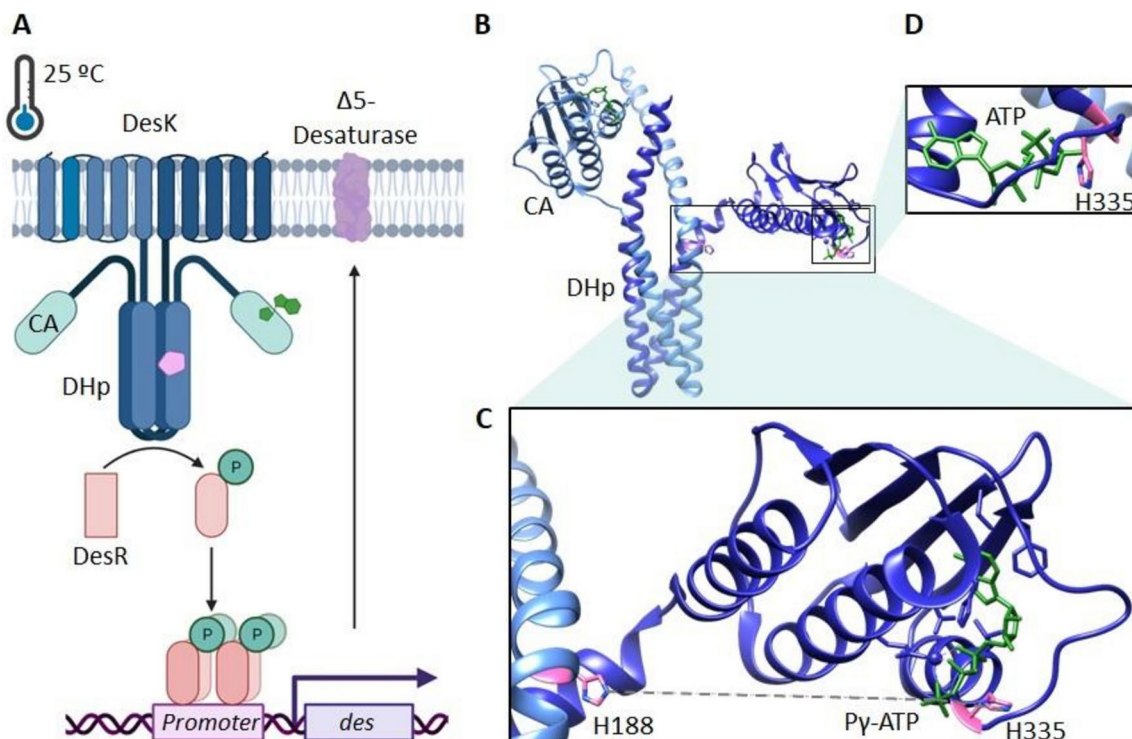


Fig. 1. Structural insights into the Histidine Kinase DesK. (A) DesK comprises a transmembrane N-terminal sensor domain, the Dimerization Histidine phosphotransfer (DHp) domain containing His 188 (represented with the pink pentagon), and the Catalytic Domain (CA) housing the ATP (in green). DesK (in blue) operates as a transmembrane sensor that detects changes in membrane properties^{21–23} triggering a cellular response aimed at maintaining membrane lipid fluidity²⁴. Under optimal growth temperatures ($\approx 37\text{ }^{\circ}\text{C}$), the membrane is thin and hydrated. In contrast, at suboptimal temperatures ($25\text{ }^{\circ}\text{C}$), the membrane turns to be thicker and dehydrated, which promotes the kinase state of DesK^{25,26}. This leads to the phosphorylation of its response regulator, DesR (reddish). Once phosphorylated, a tetramer of DesR binds to two inverted repeats in the *Pdes* promoter of the $\Delta 5$ -desaturase gene, activating its transcription^{27,28}. The $\Delta 5$ -Desaturase (in purple) catalyses the introduction of double bonds into membrane lipids to elevate levels of unsaturated fatty acids (UFAs), restoring lipid fluidity under low-temperature conditions^{29,30}. (B) Crystal structure of the dimeric phosphorylated cytoplasmic domain of DesK, DesKC, in complex with AMP-PCP (PDB 3GIG). (C) Zoom in on the rectangle shown in (B) pointing out the distance between His 188 and the AMP-PCP analogue AMP-PCP (27.7 Å). (D) Zoom in on the square shown in (B), indicating that the distance ATP—His 335 is 5.6 Å. Molecular graphics and analyses were performed with UCSF Chimera, developed by the Resource for Biocomputing, Visualization, and Informatics at the University of California, San Francisco, with support from NIH P41-GM103311.

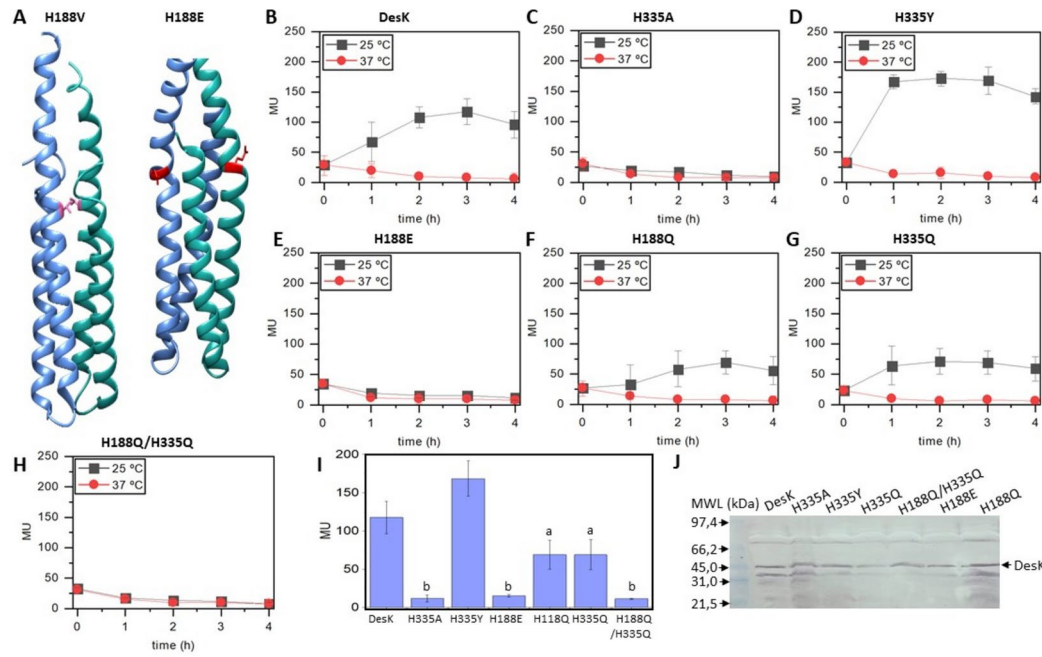


Fig. 2. Signal transduction in DesK variants. (A) Dimerization Histidine phosphotransferase (DHp) domain of H188V and H188E variants. The DHp domain is rotated inwards when the His 188 is replaced by a hydrophobic valine, highlighted in pink (PDB 3EHH). Conversely, it is rotated outwards when His 188 is substituted with a hydrophilic glutamate, highlighted in red (PDB 3GIF). (B–H) *Bacillus subtilis* Δ desK cells expressing either DesK WT and its variants H335A, H335Y, H188E, H188Q, H335Q or H188Q/H335Q were grown at 37 °C to an OD_{550} of 0.3, and then divided in two flasks. One was maintained at 37 °C (red lines), and the other transferred to 25 °C (blue lines). β -galactosidase activity was measured in Miller Units (MU). Error bars include the standard deviation from at least three independent experiments. (I) Comparison for MU for each variant at 25 °C, measured 3 h after cold shock (corresponding to one bacterial generation time post-cold shock). There is not significant difference among activities labelled with the same letter. (J) Western blots of the membrane fraction of *Bacillus* cells expressing each DesK variant show similar levels of expression and membrane integration. The band corresponding to DesK is pointed out.

| UNIPROT ID | Organism | * | 335 | * | | * | | * | * | * | * | * | * | * | * | * | |
|------------|-----------------------------------|---|----------|---|---|---|---|---|---|---|---|---|---|---|---|---|---|
| O34757 | <i>Bacillus subtilis</i> | G | H | G | L | L | G | M | R | E | R | L | E | F | A | N | G |
| A0A2N5HBF2 | <i>Neobacillus cucumis</i> | G | H | G | L | I | G | M | K | E | R | L | E | F | I | N | G |
| A0A3L7JQW3 | <i>Falsibacillus sp. GY 10110</i> | G | H | G | L | V | G | M | K | E | R | L | E | F | V | N | G |
| A0A271LZQ9 | <i>Bacillaceae bacterium</i> | G | S | G | L | L | G | M | R | E | R | L | E | F | V | N | G |
| A0A2N0ZDZ1 | <i>Cytobacillus horneckiae</i> | G | S | G | L | L | G | I | K | E | R | L | D | F | V | N | G |
| A0A094YSS6 | <i>A. alcalophilus</i> | G | Y | G | L | I | G | L | K | E | R | L | E | F | V | N | G |
| A0A559U155 | <i>Aeribacillus composti</i> | G | N | G | L | I | G | I | K | E | R | L | E | F | V | N | G |

Table 1. Homologs of DesK in different organisms. BLAST analysis was conducted to compare the amino acid sequences of the DesK homologs across multiple organisms. DesK sequence was aligned with 101 sequences. Notably, the homologous proteins exhibit a phosphorylatable residue at the equivalent position of DesK His 335 (in reference to *Bacillus subtilis*) in 70% of the cases (highlighted in bold). The asterisk (*) denotes residues that are conserved across all the 101 sequences analysed (See <https://dataVERSE.unr.edu.ar/dataset.xhtml?persistId=doi:10.57715/UNR/MPA7NB> data for the complete table).

on the signal transduction as the replacement of His 188 for valine (H188V) resulted in a protein with impaired kinase activity both in vivo and in vitro (Fig. 2A, ^{12,16,17}).

Analysing all the thirteen available DesK PDB records we observed there is a phosphorylatable residue, His 335, located at bonding distance of ATP (Fig. 1C,D). The average distance between γ P-ATP and the His 335 side-chain is 5.9 ± 0.6 Å (Table SI). It has been proposed that the short distance interaction between the side-chain nitrogen of His 335 and the γ P-ATP could play a functional role in stabilizing the ATP negative charge¹⁷. What caught our attention was that a BLAST analysis revealed that position 335 in DesK homologues was mostly occupied by phosphoryl acceptor residues and not by positively charged residues (Table 1). Likewise, HKs from

various pathogenic bacteria exhibit phosphorylatable residues in the equivalent position of His 335 of DesK (Table SII). Considering the presence of multiple phosphorylation sites in both eukaryotic and prokaryotic kinases^{18–20}, and the aforementioned facts, we wanted to investigate if His 335 could function as an alternative or redundant phosphorylation site. By this way, in the presence of a secondary phospho-acceptor, DesK could function without the conserved His 188.

In this study, we conducted a comprehensive investigation into DesK by introducing both single and double mutations. We evaluated the resulting activity of these variants both in vivo and in vitro, and further scrutinized the DesK-DesR interaction through in silico analysis across diverse DesK variants. Our studies contribute to understanding the allosteric non-canonical mechanism, which previously demonstrated that RR phosphorylation is not required. Here, we show that phosphorylation of the conserved His188 is also not required. We termed this allosteric mechanism, which does not require ATP consumption or phosphoryl transfer, as the HK-Allosteric Coupling Activation Mechanism (HK-ACAM). This work marks the first instance where a histidine kinase (HK) has been demonstrated to respond to input signals and modulate kinase activity in the absence of the DHp's conserved histidine.

Our results demonstrate that the HK EnvZ from the model Gram-negative bacterium *Escherichia coli* can also respond to its input signal in the absence of the conserved His 243 of its DHp domain. This fact suggests the unveiled HK-ACAM may be widespread among bacteria.

Results

In vivo analysis of DesK variants

To assess whether His 335 -located at \approx 5.9 Å from γ P-ATP- plays a functional role in the phosphorylation mechanism, we first replaced it with alanine, a non phosphorylatable residue typically used in mutagenesis. DesK variant H335A was cloned into the *Bacillus* replicative plasmid pHPKS, which was used to complement the *desK* mutant CM21. This strain contains the reporter gene β -galactosidase under the control of the desaturase promoter (*Pdes*) serving as a suitable host for evaluating the activation of the Des pathway by DesK^{12,31}. The kinetics and β -galactosidase levels observed in *desk* mutant strain CM21 complemented with wild-type DesK are similar to those observed in the wild-type strain AKP3^{30,31}. CM21 cells were complemented with the wild type DesK (WT-DesK) or DesK variant H335A and the activity of the reporter was measured at 25 °C or 37 °C, temperatures at which DesK is active or inactive, respectively. As expected, the control strain expressing WT-DesK showed low β -galactosidase activity at 37 °C and high at 25 °C. In contrast, the H335A mutant was not able to activate *des* expression at any temperature (Fig. 2B,C), even when it was adequately expressed and localized in the membrane fraction. This result suggests that both His 335 and His 188 could be required for efficient kinase activity.

Next, we aimed to replace His 335 for tyrosine, another residue capable of being phosphorylated. Moreover, Tyr is widely used in higher organisms signaling and is also present at the equivalent position 335 in DesK homologues (Table 1). When CM21 cells expressing variant DesK H335Y were subjected to a temperature downshift, we observed a behavior resembling that of cells expressing WT-DesK (Fig. 2D). This reinforces the idea that phosphorylation of His 335 could be a secondary phosphorylation site required for kinase activity.

Therefore, we questioned the protagonist role that has been assigned to His 188 in the activation of the DesK-DesR pathway. Up to now, the experimental evidence that points to this residue as the phosphorylatable one is based on assays showing that DesK with the mutation H188V cannot activate *des* expression in vivo and cannot undergo autophosphorylation in vitro¹². The non-conservative mutation H188V, which replaces a hydrophilic positively charged residue with a highly hydrophobic one, induces an inward rotation of the DHp. It has been proposed that this rotation, observed in the crystal structures of the cytoplasmic domain of DesK, DesKC (PDBs 3EHH and 3GIE), would shield the hydrophobic valine from water, leading to a protein lacking the kinase activity (Fig. 2A, ¹⁶). Conversely, X-ray studies performed with the cytoplasmic domain of DesK, a DesKC variant in which His 188 is replaced with glutamate, a hydrophilic residue, show that this replacement induces an outward rotation of the DHp helices¹⁶ (Fig. 2A) positioning the hydrophilic glutamate facing the solvent (PDB 3GIF). Nevertheless, the effect of this replacement had not been tested for in vivo activity in the full-length protein. We reasoned that given that the mutation H188E generates the opposite rotation of the DHp regarding valine, DesK H188E could potentially adopt a kinase-on conformation promoting DesR activation. Therefore, to test if a DesK variant whose DHp helices are rotated outwards is active -even when lacking residue His 188- we expressed the DesK variant H188E in vivo as we described above for the other mutants. The activity of DesK H188E was null both at 25 °C and 37 °C (Fig. 2E), suggesting again that either His 188 is crucial for kinase catalysis or that the replacement H188E is disruptive, setting DesK in a conformation incompatible with kinase activity. We then looked for a mutation that could substitute His 188, while conserving the appropriate structure and flexibility. Since it has been proposed that rotation of coiled coils is the essence of HK signal transduction because a cogwheel rotation is required for conformational flexibility during catalysis³², we reasoned that a non-phosphorylatable residue with amphipathic properties at position 188 would facilitate reversible helix rotation, uncovering in case there exists an alternative mechanism of activation. To investigate this, we introduced the mutation H188Q. Glutamine is a non-phosphorylatable residue that contains both a hydrophobic carbon chain and hydrophilic amide groups in the same molecule.

Surprisingly, DesK H188Q yielded an active protein capable of transmitting information, even in the absence of the conserved phosphoryl acceptor residue His 188. This variant maintains 59% of β -galactosidase activity compared to the WT at 25 °C, and it followed the same temperature dependence as the wild-type receptor (Fig. 2F).

At this point we hypothesized that there may be two phosphorylatable histidine residues, His 188 and His 335, which can transfer the phosphoryl group to the RR using alternative or redundant pathways likely to ensure DesK activity. The possible activating mechanisms are depicted in Fig. 3: In the classical phosphorylation-

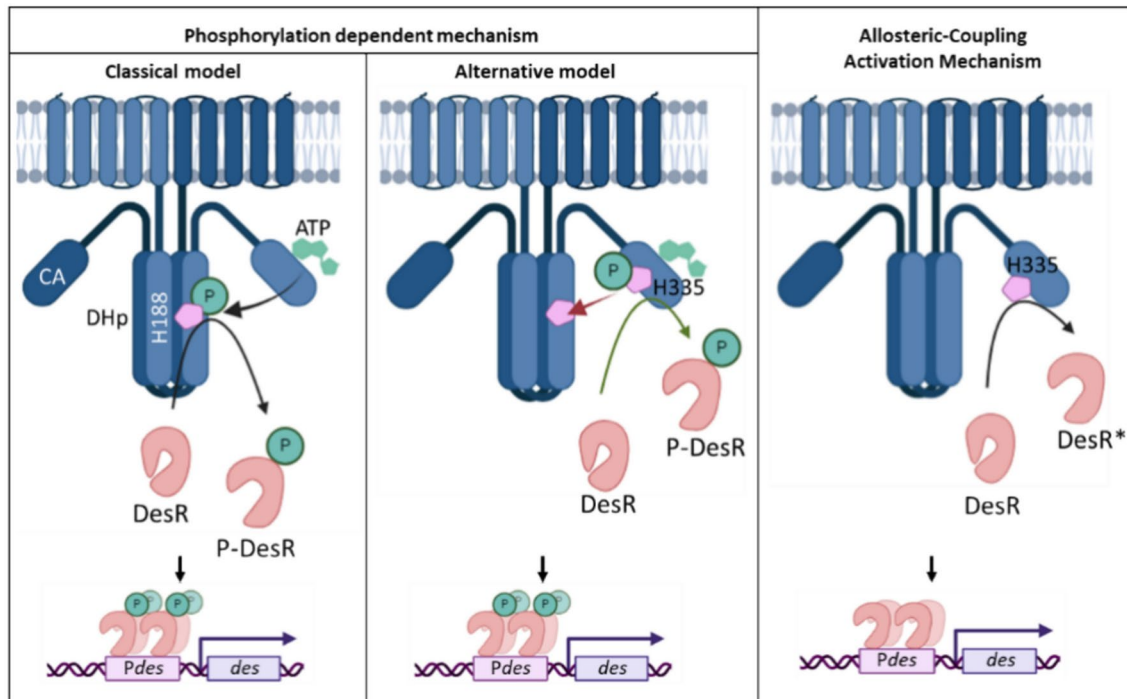


Fig. 3. DesK alternative activation mechanisms. Left panel: The phosphorylation-mediated activation involves phosphorylation of the conserved His 188 (indicated with a pink pentagon in the DHp domain), which receives the phosphate group from the ATP (highlighted in green) located in the Catalytic Domain (CA). Then, the phosphoryl group is transferred from His 188 to the Response Regulator (reddish form). Central panel: Conversely, in the alternative phosphorylation mechanism, His 335 (indicated with a pink pentagon) receives the phosphoryl group from the ATP located in the Catalytic Domain (CA). Then, the phosphoryl group may be transferred from His 335 to the His 188 (red arrow) or directly to the Response Regulator (green arrow). Right panel: A third possibility to activate DesR is the allosteric activation in the absence of autophosphorylation. The figure was created with BioRender.com.

mediated activation, the phosphoryl group is transferred from ATP to His 188, and then to the RR (Fig. 3 left panel). In the alternative phosphorylation-mediated mechanism, the phosphoryl group is transferred from ATP to His 335. Phosphorylated His 335 may directly transfer the phosphoryl group to the RR, or undergo an intramolecular phosphotransfer passing the P-group first to His 188 and subsequently to the RR (Fig. 3 central panel).

To analyze whether phosphorylation of His 335 is required in catalysis, we introduced the H335Q mutation. This choice was based on the rationale that glutamine (Q) rendered an active sensor when replacing His 188 suggesting that it preserves the necessary flexibility for DesK functionality. If His 335 phosphorylation is indeed mandatory, the DesK with the replacement H335Q should be inactive. Therefore, we cloned and expressed the DesK H335Q variant *in vivo* using the same procedures as described above. Cells expressing DesK H335Q showed activation of *Pdes* transcription at low temperature but not at high temperatures, resembling the action of the WT sensor (Fig. 2G). This result suggests, on the one hand, that phosphorylation of His 335 is not strictly required for activity provided His 188 is present and, on the other hand, that His 335 is key to DesK proper function as its replacement with a glutamine results in a 41% reduction in *Pdes* activation level, similar to the reduction in activity provoked by the substitution H188Q. Together, these findings suggest the existence of alternative pathways, one mediated by His 188 and the other by His 335.

To test this idea, we generated the double mutant H188Q/H335Q, where both His residues were substituted with glutamine. When the DesK variant H188Q/H335Q was expressed *in vivo*, the *Pdes* was inactive at both temperatures (Fig. 2H,I), even when the mutant sensor is adequately expressed and localized in the membrane fraction (Fig. 2J). The fact that the double mutant is unable to process or transmit information to DesR suggests that DesK needs either His 188 or His 335 to activate the pathway. Together, these results imply that phosphorylation of His 188 is not essential, and another activation mechanism involving His 335 must be operative in DesK.

It is noteworthy that the formation of P–N bonds in nature is relatively uncommon, and to date, glutamine residues have not been identified as phosphor-acceptors in signaling pathways. Nevertheless, it has been reported that the phosphorylation of the amide nitrogen of L-glutamine with ATP occurs during modification of the bacterial capsular polysaccharides³³. The loss of function observed in the double mutant H188Q/H335Q rules out the possibility of glutamine phosphorylation being responsible for the activity in single mutants H188Q and H335Q.

DesK in vitro phosphorylation

As we have demonstrated that His 335 plays a role in DesK signal transmission, we wanted to prove whether this residue receives the phosphoryl group from ATP as a phosphorylation intermediate. The WT soluble catalytic domain, DesKC, has been shown to autophosphorylate in vitro in the presence of $\gamma^{32}\text{P}$ -ATP. Therefore, we conducted in vitro phosphorylation assays to test our hypothesis. We cloned the soluble catalytic domain of the DesK glutamine variants, H335Q, H188Q and the double mutant H188Q/H335Q, into the pQE31 expression vector. These three His-tagged fusion proteins, as well as WT-DesKC, were expressed in *E. coli* and purified. For the in vitro phosphorylation assay, each protein was incubated at 25 °C in the presence of $\gamma^{32}\text{P}$ -ATP and aliquots were taken at different time points.

Our results indicate that WT-DesKC showed autophosphorylation and the kinase inactive protein H188Q/H335Q did not. Regarding the single variants, DesK H335Q presented autophosphorylation, but the H188Q did not, suggesting that His 335 cannot autophosphorylate (Fig. 4A). The fact that mutant DesKC H335Q was less prone to become phosphorylated than WT-DesKC (Fig. S2) agrees with the in vivo results, where variant DesK H335Q promoted lower levels of *des* expression than the WT.

The absence of autophosphorylation in the H188Q variant does not rule out the possibility that the phosphoryl group is transferred to the RR via an unstable intermediate of phosphorylated His 335 that cannot be captured in this type of in vitro assay. Therefore, we assessed whether WT-DesKC and its glutamine variants can transfer the P group to the RR¹⁶. DesKC variants were incubated with $\gamma^{32}\text{P}$ -ATP to allow autophosphorylation and then an equimolar amount of DesR was added. Figure 4B shows that DesR was phosphorylated when incubated with WT-DesKC or DesKC H335Q, but not with DesKC H188Q nor with DesKC H188Q/H335Q. Together, these experiments indicate that although autophosphorylation and phosphotransfer to DesR requires His 188, hampering His 188 phosphorylation does not prevent DesK communication: the H188Q variant is still capable

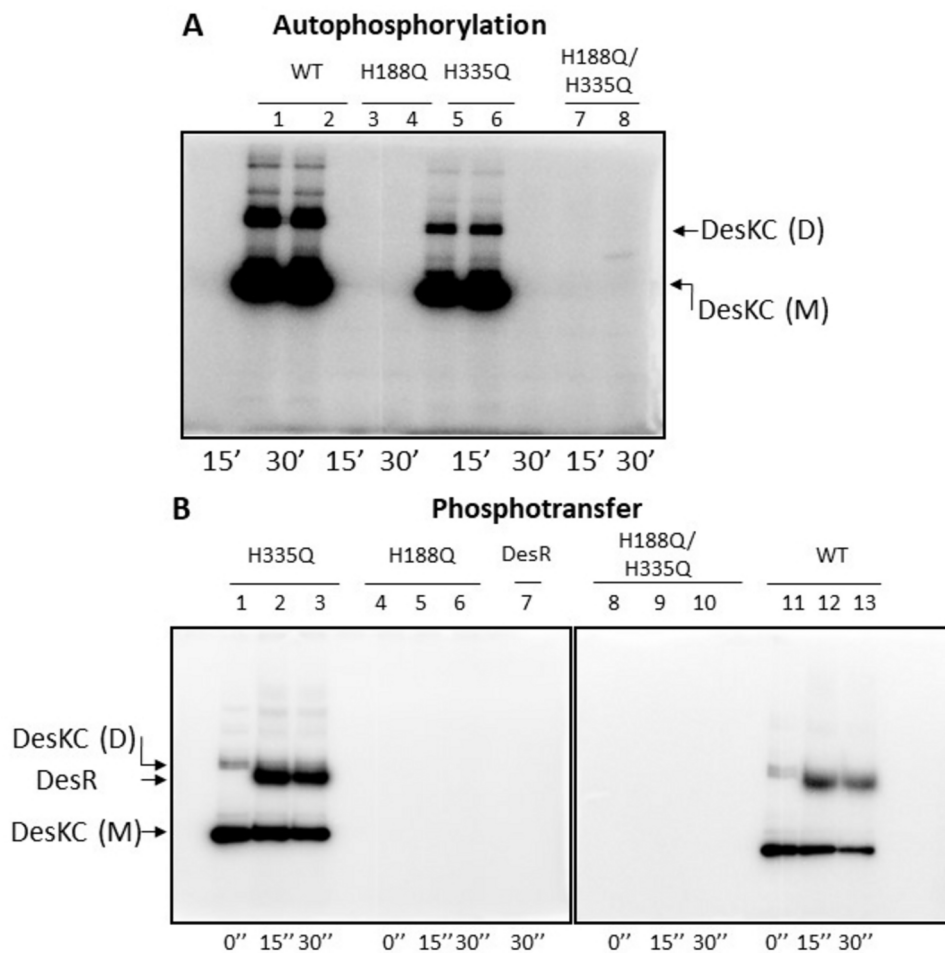


Fig. 4. Phosphorylation and end product evaluation for DesK variants. (A) In vitro autophosphorylation assay. Purified DesKC variants, WT (lanes 1–2), H188Q (lanes 3–4), H335Q (lanes 5–6) or H188Q/H335Q (lanes 7–8), were incubated with $\gamma^{32}\text{P}$ -ATP and samples were taken at 15 and 30 min. (B) Phosphotransfer to the RR. Each DesKC variant, H335Q (lanes 1–3), H188Q (lanes 4–6), H188Q/H335Q (lanes 8–10) and WT (lanes 11–13), was incubated with $\gamma^{32}\text{P}$ -ATP for 10 min and then purified GST-DesR was added. Samples were taken at 0, 15 and 30 s after addition of GST-DesR. DesR incubated with $\gamma^{32}\text{P}$ -ATP but without any DesKC variant (lane 7). (M) stands for “monomer” and (D) for “dimer”.

of activating the Des pathway at low temperatures in vivo (Fig. 2) through a phosphorylation-independent mechanism.

Unsaturated fatty acid levels in DesK variants

We measured the levels of unsaturated fatty acids in *Bacillus* cells expressing WT-DesK or its active variants H188Q and H335Q using gas chromatography-mass spectrometry (Fig. 5). Upon exposure to low temperatures, all three active strains exhibited similar levels of unsaturated fatty acids (5.65%, 4.45% and 4.17%, respectively). The fact that the expression levels of the reporter under the control of the desaturase promoter are different (Fig. 2I), but the levels of final product (unsaturated fatty acids) are similar (Table SIII) in the three strains indicates that the system is robust, meaning that the desaturase can incorporate the necessary amount of double bonds to maintain lipid homeostasis, despite variation in the desaturase protein levels.

On the contrary, when cells were grown at 37 °C, unsaturated fatty acids were absent, indicating that in fact the active proteins regulate efficiently the levels of the final product of the Des pathway in response to temperature variations (Fig. 5 and Table SIII).

Overall, our results suggest that *B. subtilis* DesK has alternative routes to transmit information to DesR. One pathway relies on phosphoryl transfer and involves His 188, while the other one is independent from His 188 phosphorylation and requires His 335 (Fig. 3 right panel).

In silico analysis of the interactions displayed by DesR and the DesK variants

The activation mechanism, independent of His 188 phosphorylation but requiring His 335, may involve allosteric binding between DesK and DesR to trigger the conformational change necessary for DesR activation. To explore the interactions involved in DesR activation in the absence of phosphorylation, we performed Molecular Dynamics Simulations (MDS) on DesR in complex with WT-DesKC, as well as its variants with either reduced or enhanced activity (H335Q and H335Y, respectively), in the absence of ATP.

DesR comprises a phosphorylatable N-terminal receiver domain (REC), consisting of six α -helices (α 1-6) and six β -sheets (β 1-6), and a C-terminal HTH domain involved in DNA binding (Fig. 6A). In its inactive form, the REC domain obstructs the access of the HTH domain to DNA. When DesK activates DesR, there is a repositioning of the two domains and release of the inhibitory effect²⁸. Such kind of regulation exerted by the N-terminus is also found in closely related response regulators, like NarL³⁴.

DesR crystal structure in the active open conformation (PDB 4LDZ) was used as the initial structure in the simulation. For DesKC, we used the coordinates obtained from the crystal structure in its active conformation, crystallized in complex with the REC domain of DesR (PDB 7SSI). We removed the coordinates for the REC domain of DesR to include full-length DesR in our simulations and removed the coordinates for the ATP molecule from DesK to emulate low ATP concentration conditions. The best full-length complex of WT DesK-DesR obtained by docking using HDOCK server³⁵ or the two derived mutants³⁶ DesK H335Q-DesR and DesK H335Y-DesR were used for MDS. In all the DesK-DesR complexes simulated DesR remained bound to DesK.

From the trajectories obtained from three independent simulations for each complex, it can be observed that, in the complex formed by WT-DesK, the DesR REC domain is orientated towards the catalytic domain of DesK (Fig. 6B): in particular, His 335 is adjacent to DesR α 2 helix (highlighted in red), and His 188 is proximate to the DesR α 1, particularly to Asp 25 (highlighted in green). The C-terminal DNA-binding domain is extended,

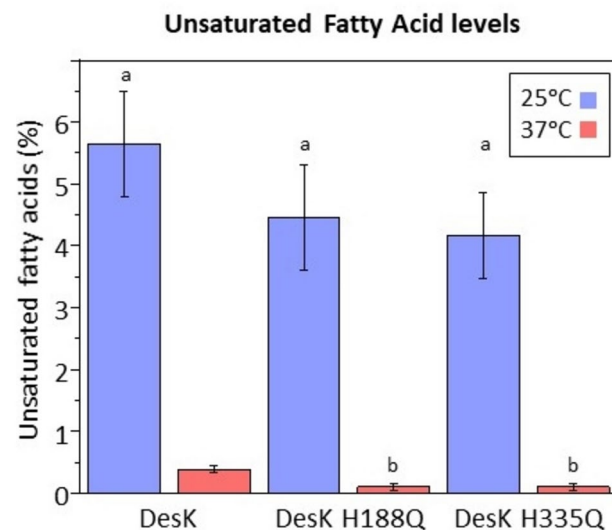


Fig. 5. Unsaturated fatty acid composition. *B. subtilis* cells expressing DesK WT, H188Q and H335Q variants were grown at 37 °C to an OD_{550} of 0.35. Cultures were split into two aliquots: one remained at 37 °C and the other was transferred to 25 °C. Total lipids were extracted and trans-esterified with sodium methoxide. The fatty-acid methyl esters were subjected to gas chromatography- coupled to a mass spectrometer.

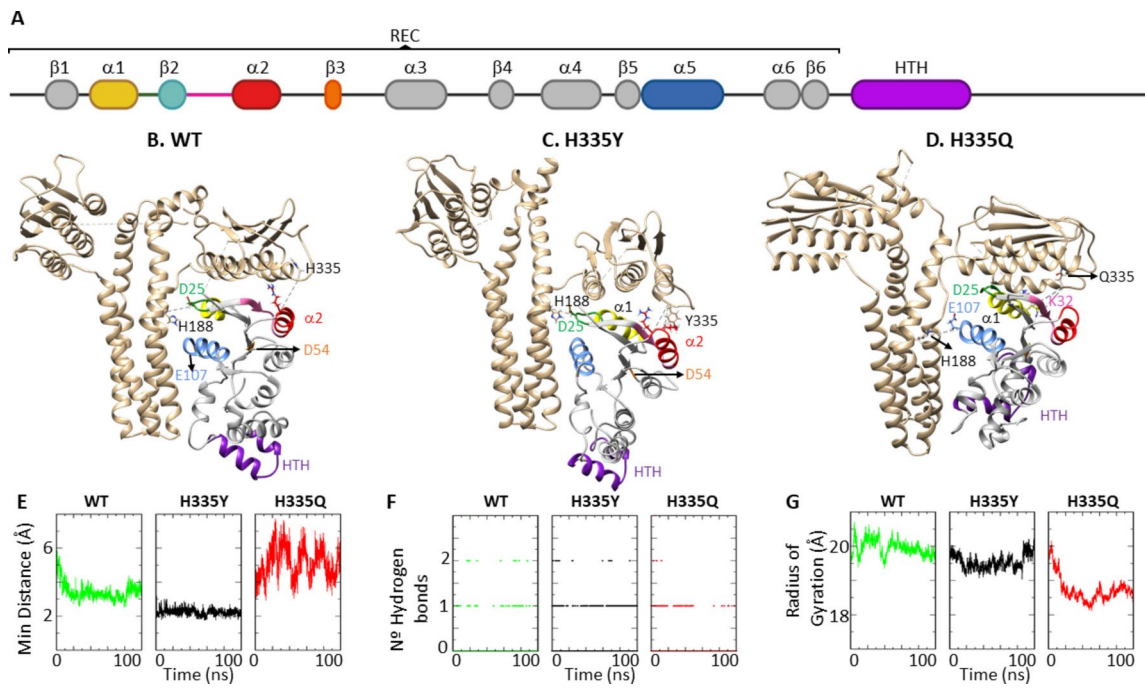


Fig. 6. MD analysis of DesR-DesK complexes. (A) Diagram of DesR indicating helices or domains mentioned in the text. (B–D) Snapshots from 100-ns molecular dynamics simulations (MDS) illustrating DesR in complexes with DesK WT, H335Y, or H335Q, respectively. (E) Minimum distance represented in Ångström (Å) between residue 335 of chain B of DesK and the regulator DesR. (F) Hydrogen bonds formed between residue 335 and DesR. (G) Radius of gyration represented in Ångström (Å) of DesR. Graphs (E–G) correspond to the average of three independent assays for each complex.

with the HTH (highlighted in violet) pointing to the solvent, compatible with the active conformation required to interact with DNA.

To analyze the behavior of the variant DesK H335Y the same procedure was applied (Fig. 6C). In the complex, DesR maintains the open orientation seen in the WT complex: Tyr 335 is close to DesR α 2 helix, and His 188 is close to DesR Asp 25. In addition, the HTH domain is even more available to interact with DNA than in the WT complex.

The same approach was performed for DesK H335Q, which is partially active in vivo, but lacks the HK-ACAM. In the DesK H335Q-DesR complex (Fig. 6D), the REC domain of DesR undergoes a general rearrangement. Here, the α 1 helix (highlighted in yellow) and the loop β 2 α 2 (highlighted in pink), containing Lys 32, moves upwards and locates close to DesK Gln 335. It is likely that this rearrangement triggers a differential folding in the rest of DesR: The C-terminal DNA-binding domain folds inwards, interacting with its N-terminal domain, diminishing exposure of the HTH domain to the DNA promoter.

We utilized the *gmx mindist* tool from GROMACS³⁷ to determine the minimum distance between His 335 of chain B in DesK and any residue of DesR. The analysis revealed that the shortest distance was observed for the DesK H335Y-DesR complex (2.3 ± 0.2 Å), which also exhibited the highest kinase activity in vivo. Conversely, the DesK H335Q-DesR complex showed the largest distance (7 ± 1 Å), corresponding to the lowest in vivo activity (Fig. 6E). The wild-type DesK-DesR complex displayed an intermediate minimum distance (4 ± 1 Å), correlating with a moderate level of activity in vivo. Minimum distances correlate with the formation of hydrogen bonds between residue 335 and DesR, as measured by *gmx hbond* (Fig. 6F).

Finally, we analyzed the radius of gyration (RG) of DesR in each complex using *gmx gyrate*. RG measures the root-mean square distance between the center of mass of the protein to its atoms, being an indicator of protein structure compactness. This parameter supports the observation that HTH acquires different degrees of solvent exposition in each complex (Fig. 6G). It can be observed that in the complexes DesK-DesR performed with the WT and the variant H335Y, variants presenting the phosphorylating and allosteric activation mechanisms, DesR has a larger radius of gyration (19.5 ± 0.1 Å), indicating that it has an extended conformation: The structure of the complex along the MDS shows that this is a consequence of the HTH domain being more extended and therefore more exposed. On the other hand, in DesK H335Q-DesR, the variant that just present the allosteric mechanism, DesR diminishes its radius of gyration (18.2 ± 0.2 Å), indicating that it has a folded, closed conformation: The structure of the complex along the MDS shows that the HTH domain's reduced exposure is responsible for this outcome.

Distinct DesK-DesR interactions occur when the DesK variants are simulated in complex with DesR: both WT and H335Y DesK variants interact with the RR keeping the active conformation in which the HTH domain remains more exposed, while variant H335Q induces a folding of the HTH favoring the inactive conformation of DesR. It should be pointed out that DesK H335Q lacks the allosteric mechanism, but can phosphorylate DesR

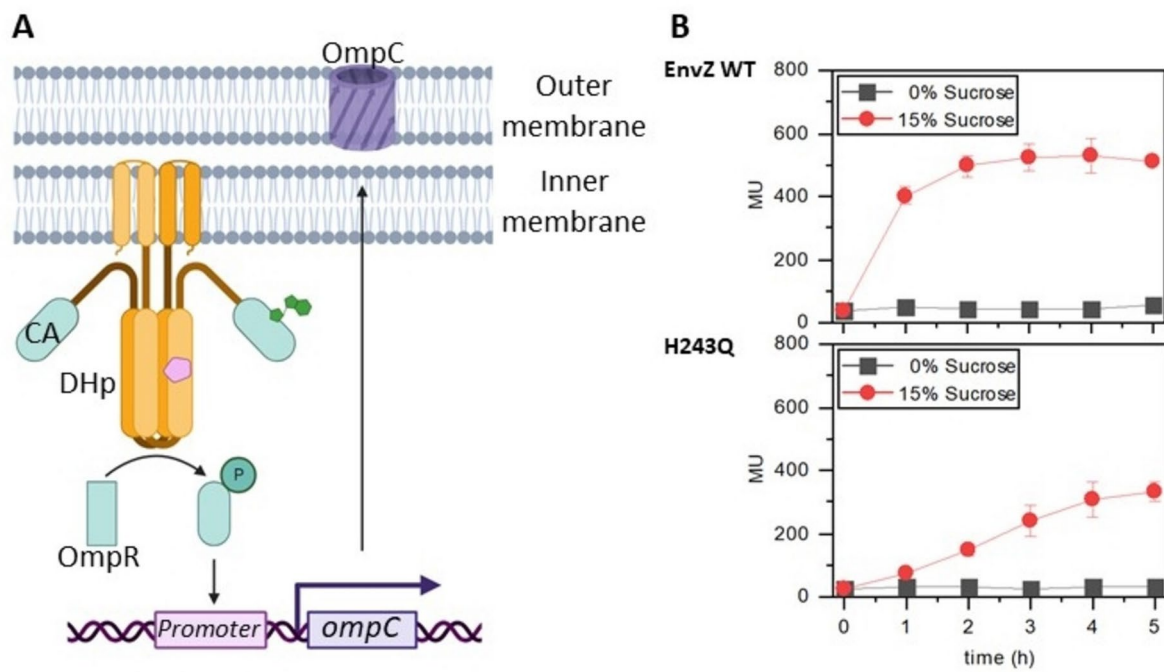


Fig. 7. Schematic Representation of the EnvZ Pathway. (A) Diagram of an EnvZ dimer situated at the inner periplasmic membrane. Its soluble domain comprises a Dimerization-Histidine phosphotransfer (DHp) domain (in orange), where the His 243 (pink pentagon) is located, and a catalytic (CA) domain housing the ATP (in green). At high osmolarity, EnvZ phosphorylates the RR OmpR, triggering the transcription of *ompC*, whose product is a porin of the outer membrane (in violet). OmpF was omitted for simplicity. (B) β -galactosidase activity from a *PompC-lacZ* reporter fusion in cells expressing the wild type EnvZ (top) or its H243Q variant (bottom) was measured at low osmolarity (Sucrose 0%, black lines) or high osmolarity (Sucrose 15%, red lines). Sucrose was added at OD_{550} of 0.3 Error bars include the standard deviation from at least three independent experiments.

and activate it chemically. Together this set of in silico studies suggests that an appropriate interaction between His 335 and DesR α 2 helix could be required for the HK-ACAM activation of DesR. However, mutagenesis of these domains is crucial to biochemically validate the in silico predicted interactions between DesK variants and DesR, providing direct evidence that these interactions are essential for the activation of DesR through the HK-ACAM mechanism.

Is HK-ACAM functional in other HKs?

We wondered whether other HKs could function when lacking the conserved histidine residue in the DHp. We focused on the osmosensor HK EnvZ, which is in the inner membrane of Gram-negative bacteria, such as *E. coli* and pathogenic *Salmonella*. At high osmolarity, EnvZ phosphorylates its corresponding RR, OmpR, to differentially upregulate porins *ompC* and repress *ompF* respectively (Fig. 7A). This regulatory pattern helps the cell maintain osmotic balance by adjusting the permeability of its outer membrane to small molecules such as ions and sugars³⁸. It is worth mentioning that in acidic conditions, OmpR is activated through a phosphorylation-independent mechanism that still requires the presence of wild type EnvZ⁸.

The EnvZ cytoplasmic domain contains the DHp domain carrying the conserved histidine identified as phosphorylatable, His 243, and encompassing a binding region for the RR OmpR, and the ATP-binding domain (Fig. 7A;³⁹). To assess activation of *ompC* expression by EnvZ, we cloned WT-EnvZ into the pBlueScript SK (+), which was used to transform the *E. coli* strain RU1012. RU1012 is mutant for EnvZ (Δ envZ::Km) and contains the reporter β -galactosidase gene fused to the promoter *ompC* (*PompC-lacZ*) so it can be complemented with different versions of the sensor to monitor the effect of mutations on the activation of *ompC* transcription. After cultivating cells expressing the WT variant at low or high osmolarity, β -galactosidase activity was measured as already reported^{40,41}. As expected, at high sucrose levels, EnvZ activated the expression of the *PompC-lacZ* reporter fusion (Fig. 7B top). To investigate if the conserved residue His 243 could be replaced by a non-phosphorylatable one, we introduced the mutation H243Q, mimicking the functional replacement performed in DesK. Strain RU1012 was complemented with this mutant and the expression of *PompC-lacZ* at high and low osmolarity was evaluated. Like WT-EnvZ, EnvZ H243Q was capable of activating transcription upon high sucrose levels, being the observed β -galactosidase activity 65% of the one obtained with the WT sensor (Fig. 7B bottom). This result demonstrates that His 243 is nonessential for EnvZ signal transduction and implies that EnvZ also harbors a phosphorylation-independent mechanism.

It is noteworthy that the replacement H243Q led to a decrease in the transcription induction level, like the reduction observed for DesK H188Q (41% for DesK and 35% for EnvZ regarding the activity achieved by their respective WT proteins). The finding that both phospho-receiving His (His 188 in DesK and His 243 in EnvZ) can be replaced by a non-phosphorylatable residue while maintaining their signal transduction capacity suggests the existence of an alternative route for HKs to activate their cognate RR independent of the conserved His and seems to be widespread among different bacteria.

Discussion

In this study, we illustrate that the signal transduction mediated by histidine kinases persists even in the absence of the conserved histidine residue within the DHp domain. Our findings suggest that an amphipathic residue at this critical position facilitates information transmission. This observation aligns with the established understanding that kinases necessitate flexibility to enable the rotation of coiled coils, crucial for catalysis and interaction with RRs⁴². Accordingly, our results contribute to elucidate why DesK mutants H188V and H188E, the first variants to be crystallized likely due to their increased structural rigidity, are inactive kinases because they lack both: (i) the canonical mechanism requiring His phosphorylation and (ii) the allosteric mechanism reliant on HK conformational flexibility.

While it has been reported that overexpression of DesR mutants lacking the phospho-acceptor Asp can adopt their active conformation in the presence of wild type DesK⁷, the present study marks the first demonstration of a HK responding to input signals and modulating the regulator's activity in the absence of the conserved DHp histidine.

Here, we present evidence that the allosteric mechanism that is independent of HK autophosphorylation, functions in two paradigmatic HKs, DesK and EnvZ. Given their roles in mediating responses to diverse environmental stimuli and belonging to model bacteria *B. subtilis* (Gram-positive) and *E. coli* (Gram-negative), our findings suggest a possible conservation of HK-ACAM across diverse bacterial Two-Component Systems (TCSs).

By comparing in vivo and in vitro activities alongside in silico studies, we propose that the interaction between the DesR α 2 helix and DesK His 335 may be necessary to elongate the RR, exposing its DNA-binding domain. Additionally, the simultaneous replacement of both His 188 and His 335 by Gln resulting in protein lacking kinase activity suggests two pathways for information transmission in DesK.

We posit that under regular conditions where ATP is available, the canonical mechanism involving autophosphorylation and subsequent phosphotransfer to the RR predominates, while under nutrient limitation or other stressful conditions, such as acidity⁸, which hinders HK autophosphorylation, HK-ACAM may become necessary.

In such circumstances, the HK retains its ability to detect the input signal, triggering the coiled-coil rotation of DHp helices required for HK activation^{21–23}. The active unphosphorylated conformation facilitates interaction with the RR enabling RR activation without phosphorylation. However, our results do not differentiate whether active but unphosphorylated DesK interacts with DesR in the closed-inactive conformation to initiate activation or stabilizes a pre-existing population of active DesR molecules preceding the input signal^{8,41,43–45}.

Our results open new avenues of investigation into the diverse signal transduction mechanisms bacteria employ for information transmission and addresses the gap between enzymes and pseudo-enzymes, which mimic enzymatic functions but operate without catalysis^{46–48}. Finally, HKs represent a widely conserved group of proteins found in yeasts, bacteria, archaea, filamentous fungi, slime molds, and plants, yet notably absent in humans. Given their role in bacterial pathogenesis, HKs offer promising targets for antibiotic development⁴⁵. Moreover, our results underscore the importance of unconventional mechanisms that bacterial and potentially human kinases may employ to transmit crucial information, bypassing classical pathways.

Experimental procedures

Mutants and strain constructions

Mutagenic oligonucleotides listed in Table SIV were used to introduce DesK mutations into the pLARC1 plasmid. This plasmid derived from pHPKS carries a xylose-inducible promoter, *Pxy*_l, which controls expression of DesK variants⁷. The resulting plasmids were utilized to transform CM21 *Bacillus subtilis* strain. This strain features a deletion in the *desK* gene and includes a transcriptional fusion where the reporter gene β -galactosidase is inserted after the promoter of the *desaturase* gene [JH642 *amyE*::P_{des}-*lacZ* (Chloramphenicol), *desKR*::Kanamycin, *thrC*::*Pxy*_l-*desR* (Spectinomycin)], facilitating the monitoring of DesK kinase activity¹².

For the EnvZ variants, wild type *envZ* was cloned into the pBlueScript SK (+) plasmid under the control of a lactose-inducible promoter. Mutagenic oligonucleotides (Table SIV) were utilized to introduce the H243Q mutation. These plasmids were employed to transform the RU1012 strain. This strain incorporates a Kanamycin resistance cassette disrupting the *envZ* gene and a fusion of the *lacZ* gene to the *ompC* promoter ([Φ(ompC-*lacZ*+10–25], Δ *envZ*::KmR, Δ (*lacZYA*-*argF*)U169, *rpsL*, *araD139*, *relA*, *thiA*, *malQ7*, *par*::*Mucts10* λ₁p1)^{40,41}.

All mutations were verified through DNA sequence analysis (MACROGEN). Strains are available upon request.

Growth conditions and in vivo kinase activity measurements

For β -galactosidase measurements, the *B. subtilis* CM21 cells complemented with the plasmids encoding the corresponding DesK variants were cultured at 37 °C in Spizizen medium until reaching an OD₅₅₀ of 0.3. Subsequently, the cultures were divided into two aliquots: one remained at 37 °C and the other was transferred to 25 °C. To induce the expression of DesK variants, 0.1% xylose was added to the growth medium. Samples were collected at 1-h-intervals and β -galactosidase activity was determined as previously described⁴⁹.

For β -galactosidase determination of cells expressing EnvZ WT or the H243Q variant, RU1012 strain cells complemented with the respective plasmids were cultured in defined medium A at 37 °C until reaching an OD₅₅₀ of 0.3. At this juncture, one aliquot was supplemented with sucrose 15%. Samples were collected at 1-h-intervals and processed as described for CM21 cells.

Western blots

B. subtilis Δ desK CM21 cells, harbouring plasmids expressing each variant, were cultivated at 37 °C in the presence of xylose 0.8% until reaching an OD₅₅₀ of 1. Subsequently, membrane and cytoplasmic fractions were separated through ultracentrifugation at 45,000 g. Membranes were resuspended in buffer Tris 50 mM, NaCl 100 mM, and a SDS-PAGE was conducted as a loading control to adjust protein content (Fig. S1). Then, samples were subjected to analysis via Western blot using Anti-DesKC rabbit polyclonal antibodies.

Analysis of fatty acids by GC-MS

To determine the fatty acid composition, *B. subtilis* CM21 cells complemented with plasmids encoding DesK variants (WT, H188Q and H335Q) were grown in Spizizen minimal medium with glycerol as carbon source and 0.1% xylose as inductor at 37 °C to an OD₅₅₀ of 0.35. Cultures were split into two aliquots: one remained at 37 °C and the other was transferred to 25 °C. After 5 h of growth, 50 mL-sample-cultures were collected and lipids were extracted according to the Bligh and Dyer method⁵⁰. The fatty acids (FA) methyl esters were prepared by transesterification of glycerolipids with 0.5 M sodium methoxide in methanol⁵¹ and were analyzed in an Agilent 7890B Mass gas chromatography- coupled to a mass spectrometer Agilent 5977A on a capillary column HP-88 (100 m \times 0.25 mm con 0.20 μ m). Branched chain FA, straight-chain FA, and UFA used as reference compounds were obtained from Sigma Chemical Co.

In vitro phosphorylation analysis

These assays were carried out essentially as described in¹². For autokinase activity, 10 μ M of purified His tagged-DesKC variants (WT, H188Q, H335Q, H188Q/H335Q) were incubated for various time periods in R buffer (50 mM Tris pH 8, 200 mM NaCl, 1 mM dithiothreitol, 20% glycerol, 50 mM KCl, 1 mM MgCl₂) containing 25 μ M ATP in the presence of 0.25 μ Ci of γ^{32} P-ATP/ μ l (Easytides-Perkin Elmer). The phosphotransfer assays were carried out by first allowing DesKC variants (10 μ M) to be autophosphorylated for 10 min in 150 μ l of R buffer and then adding an equal volume of 10 μ M purified GST-DesR in R buffer. Before adding GST-DesR, an aliquot of 15 μ l corresponding to time zero was withdrawn. After the addition of GST-DesR, 30- μ l aliquots were withdrawn at various time points. Then, the samples were subjected to SDS-PAGE on 12% polyacrylamide gels. After electrophoresis, the gels were dried, exposed to a radioactive storage screen and analysed using an Amersham Biosciences Molecular Dynamics Typhoon™ FLA 7000 scanner.

Docking and molecular dynamics simulation

To obtain a full-length complex of DesK-DesR we performed protein–protein docking using HDOCK³⁵ server. The input structures consisted of DesK structure in the phosphotransfer state (PDB 7SSI)⁵², where the H188E mutation was reverted to its WT, and the full-length DesR in the active state (PDB 4LDZ)⁷. The best model obtained from the HDOCK result was selected as a starting structure for MD simulations. This complex is denominated WT-DesK-DesR.

This full-length DesK-DesR complex obtained was used to generate two complexes where the DesK histidine residue 188 was alternatively mutated to glutamine and tyrosine, generating two mutated complexes DesK H335Q-DesR and DesK H335Y-DesR. All mutations were performed using the mutation wizard tool in Pymol³⁶.

These three complexes were used as starting structures to perform MD simulations in aqueous phase, to assess complex stability and determine the key residues in protein–protein interactions. All-atom MD simulations of each of these systems were performed in triplicate, for 100 ns using GROMACS v.2020 with GPU acceleration³⁷, and Amber99sb force field⁵³. The box size was set at approximately 146 \times 146 \times 146 \AA . These systems were solvated using the TIP3P water model⁵⁴ and chloride and sodium ions were added to neutralize the system. First, an energy minimization was performed using steepest descent, using 10,000 steps and an integration step of 2 fs. The temperature and pressure were kept constant at 300 K and 1 bar, with a V-rescale thermostat and Berendsen barostat, respectively, resulting in a NPT ensemble (constant number of molecules, pressure and temperature). Electrostatic interactions were treated using PME and a rcoulomb was set to 1 \AA . An isotropic pressure coupling was used, with a compression constant of 1 bar, and a compressibility module 4.5e⁻⁵. All bonds were constraints using the LINCS algorithm⁵⁵.

MD trajectories were analyzed using the GROMACS TOOL package³⁷. We calculated the radius of gyration using the program gmx gyrate, which gives a measure for the compactness of a structure. The minimum distance between two groups of atoms was calculated with the program gmx mindist. Hydrogen bonds were calculated with gmx hbond using the geometrical criterion of a donor–acceptor distance of 0.35 nm and an angle of 30°.

Statistical analysis

A comparison of β -galactosidase activity for DesK variants at 25 °C was conducted using ANOVA to determine the statistical significance of the differences among the measurements. A nonparametric test was employed with a significance threshold set at p value < 0.05 .

Data availability

The datasets generated and during the current study are available in the repository of the Universidad Nacional de Rosario (UNR), <https://dataVERSE.unr.edu.ar/dataset.xhtml?persistentId=doi:10.57715/UNR/MPA7NB>.

Received: 9 October 2024; Accepted: 28 January 2025

Published online: 26 April 2025

References

- Zschiedrich, C. P., Keidel, V. & Szurmant, H. Molecular mechanisms of two-component signal transduction. *J. Mol. Biol.* **428**, 3752–3775 (2016).
- Papon, N. & Stock, A. M. Quick guide. Two-component systems. *Curr. Biol.* **29**, R724–R725 (2019).
- Bourret, R. B. Receiver domain structure and function in response regulator proteins. *Curr. Opin. Microbiol.* **13**, 142–149 (2010).
- Gao, R. & Stock, A. Biological insights from structures of two-component proteins. *Annu. Rev. Microbiol.* **63**, 133–154 (2009).
- Volkman, B. F., Lipson, D., Wemmer, D. E. & Kern, D. Two-state allosteric behavior in a single-domain signaling protein. *Science* **291**, 2429–2433 (2001).
- Buschiazza, A. & Trajtenberg, F. Two-component sensing and regulation: How do histidine kinases talk with response regulators at the molecular level? *Annu. Rev. Microbiol.* **73**, 507–528 (2019).
- Trajtenberg, F. et al. Allosteric activation of bacterial response regulators: The role of the cognate histidine kinase beyond phosphorylation. *MBio* <https://doi.org/10.1128/mBio.02105-14> (2014).
- Chakraborty, S., Winardhi, R. S., Morgan, L. K., Yan, J. & Kenney, L. Non-canonical activation of OmpR drives acid and osmotic stress responses in single bacterial cells. *Nat. Commun.* **8**, 1587 (2017).
- Desai, S. K. & Kenney, L. J. To~P or Not to~P? Non-canonical activation by two-component response regulators. *Mol. Microbiol.* **103**, 203–213 (2017).
- Roberts, D. L., Bennett, D. W. & Forst, S. A. Identification of the site of phosphorylation on the osmosensor, EnvZ, of *Escherichia coli*. *J. Biol. Chem.* **269**, 8728–8733 (1994).
- Wang, L. C., Morgan, L. K., Godakumbura, P., Kenney, L. J. & Anand, G. S. The inner membrane histidine kinase EnvZ senses osmolarity via helix-coil transitions in the cytoplasm. *EMBO J.* **31**, 2648–2659 (2012).
- Albanesi, D., Mansilla, M. C. & de Mendoza, D. The membrane fluidity sensor DesK of *Bacillus subtilis* controls the signal decay of its cognate response regulator. *J. Bacteriol.* **186**, 2655–2663 (2004).
- Devi, S. N., Kiebler, B., Haggatt, L. & Fujita, M. Evidence that autophosphorylation of the major sporulation kinase in *Bacillus subtilis* is able to occur in trans. *J. Bacteriol.* **197**, 2675–2684 (2015).
- Goodman, A. L. et al. Direct interaction between sensor kinase proteins mediates acute and chronic disease phenotypes in a bacterial pathogen. *Genes Dev.* **23**, 249–259 (2009).
- Fabret, C., Feher, V. A. & Hoch, J. A. Two-component signal transduction in *Bacillus subtilis*: How one organism sees its world. *J. Bacteriol.* **181**, 1975–1983 (1999).
- Albanesi, D. et al. Structural plasticity and catalysis regulation of a thermosensor histidine kinase. *Proc. Natl. Acad. Sci.* **106**, 16185–16190 (2009).
- Trajtenberg, F., Graña, M., Ruéalo, N., Botti, H. & Buschiazza, A. Structural and enzymatic insights into the ATP binding and autophosphorylation mechanism of a sensor histidine kinase. *J. Biol. Chem.* **285**, 24892–24903 (2010).
- Teran-Melo, J. L. et al. Routes of phosphoryl group transfer during signal transmission and signal decay in the dimeric sensor histidine kinase ArcB. *J. Biol. Chem.* **293**, 13214–13223 (2018).
- Chu, N. et al. Akt kinase activation mechanisms revealed using protein semisynthesis. *Cell.* **174**, 897–907.e14 (2018).
- Venta, R. et al. A processive phosphorylation circuit with multiple kinase inputs and mutually diversional routes controls G1/S decision. *Nat. Commun.* <https://doi.org/10.1038/s41467-020-15685-z> (2020).
- Cybulski, L. E., Martín, M., Mansilla, M. C., Fernández, A. & De Mendoza, D. Membrane thickness cue for cold sensing in a bacterium. *Curr. Biol.* **20**, 1539–1544 (2010).
- Inda, M. E. et al. Driving the catalytic activity of a transmembrane thermosensor kinase. *Cell. Mol. Life Sci.* **77**, 3905–3912 (2019).
- Almada, J. C. et al. Interhelical h-bonds modulate the activity of a polytopic transmembrane kinase. *Biomolecules* **11**, 1–12 (2021).
- Cybulski, L. E. et al. Mechanism of membrane fluidity optimization: Isothermal control of the *Bacillus subtilis* acyl-lipid desaturase. *Mol. Microbiol.* **45**, 1379–1388 (2002).
- Cybulski, L. E. et al. Activation of the bacterial thermosensor DesK involves a serine zipper dimerization motif that is modulated by bilayer thickness. *Proc. Natl. Acad. Sci. U. S. A.* **112**, 6353–6358 (2015).
- Inda, M. E., Oliveira, R. G., de Mendoza, D. & Cybulski, L. E. The single transmembrane segment of minimal sensor DesK senses temperature via a membrane-thickness caliper. *J. Bacteriol.* **198**, 2945–2954 (2016).
- Cybulski, L. E., Del Solar, G., Craig, P. O., Espinosa, M. & de Mendoza, D. *Bacillus subtilis* DesR functions as a phosphorylation-activated switch to control membrane lipid fluidity. *J. Biol. Chem.* **279**, 39340–39347 (2004).
- Najle, S. R., Inda, M. E., de Mendoza, D. & Cybulski, L. E. Oligomerization of *Bacillus subtilis* DesR is required for fine tuning regulation of membrane fluidity. *Biochim. Biophys. Acta Gen. Subj.* **1790**, 1238–1243 (2009).
- Altabe, S. G., Aguilar, P., Caballero, G. M. & de Mendoza, D. The *Bacillus subtilis* acyl lipid desaturase is a $\Delta 5$ desaturase. *J. Bacteriol.* **185**, 3228–3231 (2003).
- Aguilar, P. S., Hernandez-Arriaga, A. M., Cybulski, L. E., Erazo, A. C. & de Mendoza, D. Molecular basis of thermosensing: A two-component signal transduction thermometer in *Bacillus subtilis*. *EMBO J.* **20**, 1681–1691 (2001).
- Porrini, L., Cybulski, L. E., Altabe, S. G., Mansilla, M. C. & de Mendoza, D. Cerulenin inhibits unsaturated fatty acids synthesis in *Bacillus subtilis* by modifying the input signal of DesK thermosensor. *Microbiologyopen* **3**, 213–224 (2014).
- Abriata, L. A., Albanesi, D., Dal Peraro, M. & de Mendoza, D. Signal sensing and transduction by histidine kinases as unveiled through studies on a temperature sensor. *Acc. Chem. Res.* **50**, 1359–1366 (2017).
- Taylor, Z. W. et al. Discovery of a glutamine kinase required for the biosynthesis of the O-methyl phosphoramidate modifications found in the capsular polysaccharides of *Campylobacter jejuni*. *J. Am. Chem. Soc.* **139**, 9463–9466 (2017).
- Katsir, G., Jarvis, M., Phillips, M., Ma, Z. & Gunsalus, R. P. The *Escherichia coli* NarL receiver domain regulates transcription through promoter specific functions. *BMC Microbiol.* **15**, 1–13 (2015).
- Yan, Y., Tao, H., He, J. & Huang, S. Y. The HDOCK server for integrated protein–protein docking. *Nat. Protoc.* **15**, 1829–1852 (2020).
- Schrödinger, L. & DeLano, W. PyMOL (2020). Retrieved from <http://www.pymol.org/pymol>.
- Abraham, M. J. et al. Gromacs: High performance molecular simulations through multi-level parallelism from laptops to supercomputers. *SoftwareX* **1–2**, 19–25 (2015).
- Kenney, L. J. & Anand, G. S. EnvZ/OmpR two-component signaling: An archetype system that can function noncanonically. *EcoSal Plus* <https://doi.org/10.1128/ecosalplus.esp-0001-2019> (2020).
- Qin, L., Cai, S., Zhu, Y. & Inouye, M. Cysteine-scanning analysis of the dimerization domain of EnvZ, an osmosensing histidine kinase. *J. Bacteriol.* **185**, 3429–3435 (2003).
- Utsumi, R. et al. Activation of bacterial porin gene expression by a chimeric signal transducer in response to aspartate. *Science* **245**, 1246–1249 (1989).
- Blain, K. Y., Kwiatkowski, W. & Choe, S. The functionally active mistic-fused histidine kinase receptor. *EnvZ. Biochem.* **49**, 9089–9095 (2010).
- Saita, E. et al. A coiled coil switch mediates cold sensing by the thermosensory protein DesK. *Mol. Microbiol.* **98**, 258–271 (2015).
- Changeux, J. P. Allostery and the Monod-Wyman-Changeux model after 50 years. *Annu. Rev. Biophys.* **41**, 103–133 (2012).

44. Imelio, J. A., Trajtenberg, F. & Buschiazzo, A. Allostery and protein plasticity: The keystones for bacterial signaling and regulation. *Biophys. Rev.* **13**, 943–953 (2021).
45. Eguchi, Y. et al. Angucycline antibiotic waldiomycin recognizes common structural motif conserved in bacterial histidine kinases. *J. Antibiot.* **70**, 251–258 (2017).
46. Vaughan-Hirsch, J. et al. Function of the pseudo phosphotransfer proteins has diverged between rice and *Arabidopsis*. *Plant J.* **106**, 159–173 (2021).
47. Jeffery, C. J. Enzymes, pseudoenzymes, and moonlighting proteins: Diversity of function in protein superfamilies. *FEBS J.* **287**, 4141–4149 (2020).
48. Collins, M. J. & Childers, W. S. The upcycled roles of pseudoenzymes in two-component signal transduction. *Curr. Opin. Microbiol.* **61**, 82–90 (2021).
49. Miller, J. H. *Experiments in Molecular Genetics* (Cold Spring Harb Lab, 1972).
50. Bligh, E. G. & Dyer, W. J. A rapid method of total lipid extraction and purification. *Can. J. Biochem. Physiol.* **37**(8), 911–917 (1959).
51. Christie, W. W. & Breckenridge, G. H. M. G. Separation of cis and trans isomers of unsaturated fatty acids by high-performance liquid chromatography in the silver ion mode. *J. Chromatogr. A.* **469**, 261–269 (1989).
52. Lima, S. et al. An allosteric switch ensures efficient unidirectional information transmission by the histidine kinase DesK from *Bacillus subtilis*. *Sci. Signal.* <https://doi.org/10.1126/scisignal.abo7588> (2023).
53. Hornak, V. et al. Comparison of multiple amber force fields and development of improved protein backbone parameters. *Proteins Struct. Funct. Bioinforma* **65**, 712–725 (2006).
54. Jorgensen, W. L., Chandrasekhar, J., Madura, J. D., Impey, R. W. & Klein, M. L. Comparison of simple potential functions for simulating liquid water. *J. Chem. Phys.* **79**, 926–935 (1983).
55. Hess, B., Bekker, H., Berendsen, H. J. & Fraaije, J. G. LINCS: A linear constraint solver for molecular simulations. *J. Comput. Chem.* **18**, 1463–1472 (1997).

Acknowledgements

A.B., V.M., D.A. and L.C. are Career Investigators from the National Scientific and Technical Research Council of Argentina (CONICET). L.P. is a postdoctoral fellow from the National Agency for the Promotion of Science and Technology in Argentina (ANPCyT). J.C.A acknowledges a doctoral fellowship from CONICET. This work was supported by grants PIP2020-1862 (CONICET) and PICT2020-01034 (ANPCyT) to Dr. Cybulski and PICT 2019-00694 (ANPCyT) to Dr. Albanesi.

Author contributions

J.C.A.: Investigation, methodology, writing, review, editing. A.B.: Investigation, methodology, writing, review, editing. L.P.: Investigation, methodology, D.A.: Investigation, methodology, V.M.: Investigation, methodology, software, L.E.C.: Conceptualization; Investigation; Funding acquisition; original draft; writing, review & editing.

Declarations

Competing interests

The authors declare no competing interests.

Additional information

Supplementary Information The online version contains supplementary material available at <https://doi.org/10.1038/s41598-025-88468-5>.

Correspondence and requests for materials should be addressed to L.C.

Reprints and permissions information is available at www.nature.com/reprints.

Publisher's note Springer Nature remains neutral with regard to jurisdictional claims in published maps and institutional affiliations.

Open Access This article is licensed under a Creative Commons Attribution-NonCommercial-NoDerivatives 4.0 International License, which permits any non-commercial use, sharing, distribution and reproduction in any medium or format, as long as you give appropriate credit to the original author(s) and the source, provide a link to the Creative Commons licence, and indicate if you modified the licensed material. You do not have permission under this licence to share adapted material derived from this article or parts of it. The images or other third party material in this article are included in the article's Creative Commons licence, unless indicated otherwise in a credit line to the material. If material is not included in the article's Creative Commons licence and your intended use is not permitted by statutory regulation or exceeds the permitted use, you will need to obtain permission directly from the copyright holder. To view a copy of this licence, visit <http://creativecommons.org/licenses/by-nc-nd/4.0/>.

© The Author(s) 2025